Carbonate delta drift

Lüdmann, Thomas; Betzler, Christian; Eberli, Gregor P.; Reolid, Jesús; Reijmer, John J.G.; Sloss, Craig R.; Bialik, Or M.; Alvarez-Zarikian, Carlos A.; Alonso-García, Montserrat; Blättler, Clara L.; Guo, Junhua Adam; Haffen, Sébastien; Horozal, Senay; Inoue, Mayuri; Jovane, Luigi; Kroon, Dick; Lanci, Luca; Laya, Juan Carlos; Mee, Anna Ling Hui; Nakakuni, Masatoshi

published in
Marine Geology

2018

DOI (link to publisher)
10.1016/j.margeo.2018.04.011

document version
Publisher's PDF, also known as Version of record

Marine Geology 401 (2018) 98–111

Contents lists available at ScienceDirect

Marine Geology

journal homepage: www.elsevier.com/locate/margo

Carbonate delta drift: A new sediment drift type

Thomas Lüdmann[a,*], Christian Betzler[a], Gregor P. Eberli[b], Jesús Reolid[a], John J.G. Reijmer[c], Craig R. Sloss[d], Or M. Bialik[e], Carlos A. Alvarez-Zarikian[f], Montserrat Alonso-García[g,h], Clara L. Blättler[i], Junhua Adam Guo[j], Sébastien Haffen[k], Senay Horozal[l], Mayuri Inoue[m], Luigi Jovane[n], Dick Kroon[o], Luca Lanci[p], Juan Carlos Laya[q], Anna Ling Hui Mee[b], Masatoshi Nakakuni[r], B. Nagender Nath[s], Kaoru Niino[t], Loren M. Petruny[u], Santi D. Pratiwi[v], Angela L. Slagle[w], Xiang Su[x], Peter K. Swart[b], James D. Wright[y], Zhengquan Yao[z,aa], Jeremy R. Young[ab]

[a] Institute of Geology, CEN, University of Hamburg, Bundesstrasse 55, Hamburg 20146, Germany
[b] Department of Marine Geosciences, Rosenstiel School of Marine & Atmospheric Science, University of Miami, Miami, FL 33149, USA
[c] College of Petroleum Engineering and Geosciences, Fahd University of Petroleum and Minerals, Dhahran 31261, Saudi Arabia
[d] Earth and Environmental Sciences, University of Technology Queensland, R-Block 317, 2 George Street, Brisbane, Queensland 4001, Australia
[e] Dr. Moses Strauss Department of Marine Geosciences, The Leon H. Charney School of Marine Sciences, University of Haifa, Carmel 31905, Israel
[f] International Ocean Discovery Program, Texas A&M University, Discovery Drive, College Station, TX 77845, USA
[g] Instituto Portugues do Mar e da Atmosfera (IPMA), Divisão de Geologia e Georecursos Marinhos, Rua Alfredo Magalhães Ramalho, 6, 1495-006, Portugal
[h] Centro de Ciencias do Mar (CCMAR), Universidade do Algarve, Faro, Portugal
[i] Department of Geosciences, Princeton University, Guyot Hall, Princeton, NJ 08544, USA
[j] Department of Geological Sciences, California State University Bakersfield, 9001 Stockdale Highway, Bakersfield, CA 93311, USA
[k] Physical Properties Specialist, Ecole Nationale Superieure de Geologie, Universite de Lorraine, 2 rue du Doyen Marcel Roubault, Vandoeuvre-les-Nancy 54501, France
[l] Petroleum and Marine Research Division, Korea Institute of Geoscience & Mineral Resources (KIGAM), Gwahang-no 124, Yuseong-gu, Daejeon 305-350, Republic of Korea
[m] Graduate School of Natural Science and Technology, Okayama University, 3-1-1 Tsushima-naka, 700-8530, Japan
[n] Instituto Oceanográfico da Universidade de São Paulo, Praça do Oceanográfico, 191, São Paulo, SP 05508-120, Brazil
[o] School of GeoSciences, University of Edinburgh, Grant Institute, The King's Buildings, James Hutton, Edinburgh EH9 3FE, United Kingdom
[p] Istituto di Scienze della Terra, Università di Urbino, Via S. Chiara 27, Urbino 61029, Italy
[q] Department of Geology and Geophysics, Texas A&M University, Mail Stop 3115, College Station, TX 77843-3115, USA
[r] Department of Environmental Engineering for Symbiosis, Soka University, 1-236 Tangi-cyo, Hachioji-shi, Tokyo 192-0003, Japan
[s] Geological Oceanography Division, CSIR-National Institute of Oceanography, Dona Paula, Goa 403004, India
[t] Graduate School of Science and Engineering, Yamagata University, 1-4-12 Kojirakawa-machi, Yamagata City 990-8560, Japan
[u] Environmental Science and Policy Department, David King Hall Rm 3005, MSN 5F2, George Mason University, University Drive, Fairfax, VA 22030-4444, USA
[v] Universitas Padjadjaran, Geological Engineering, Jl. Raya Bandung, Sumedang KM 21, Jatinangor 45363, Indonesia
[w] Lamont-Doherty Earth Observatory, Columbia University, Borehole Bldg. 61 Route 9W, Palisades, NY 10964, USA
[x] Key Laboratory of Marginal Sea Geology, South China Sea Institute of Oceanology, Chinese Academy of Sciences, West Xingang Road, Guangzhou 510301, PR China
[y] Department of Geological Sciences, Rutgers, The State University of New Jersey, 610 Taylor Road, Piscataway, NJ 08854-8066, USA
[z] Department of Marine Geology, First Institute of Oceanography (FIO) State Oceanic Administration (SOA), #6 Xian Xia Ling Road, Qingdao, Shandong Province 266061, PR China
[aa] Laboratory for Marine Geology, Qingdao National Laboratory for Marine Science and Technology, Qingdao, PR China
[ab] Department of Earth Sciences, University College London, Gower Street, London, WC1E 6BT, United Kingdom

ARTICLE INFO

Editor: Michele Rebesco

Keywords:
Delta drift
Carbonate platform
Drift sedimentation
Bottom current
Clinoform
Maldives

ABSTRACT

Based on high-resolution reflection seismic and core data from IODP Expedition 359 we present a new channel-related drift type attached to a carbonate platform slope, which we termed delta drift. Like a river delta, it is comprised of several stacked lobes and connected to a point source. The delta drifts were deposited at the exit of two gateways that connect the Inner Sea of the Maldives carbonate platform with the open ocean. The channels served as conduits focusing and accelerating the water flow; Entrained material was deposited at their mouth where the flows relaxed. The lobe-shaped calcareous sediment drifts must have formed under persistent water through flow. Sediment supply was relatively high and continuous, resulting in an average sedimentation rate of 17 cm ka^{-1}. The two delta drifts occupy 342 and 384 km^2, respectively; with a depositional relief of

* Corresponding author.
E-mail address: thomas.luedmann@uni-hamburg.de (T. Lüdmann).

https://doi.org/10.1016/j.margeo.2018.04.011
Received 2 June 2017; Received in revised form 18 April 2018; Accepted 19 April 2018
Available online 23 April 2018
0025-3227/

approximately 500 m. They have a sigmoidal clinoform reflection pattern with a particular convex upward bending of the foresets. In the Maldives the drift onset marks the transition from a sea-level controlled to a progressively current dominated depositional regime. This major event occurred in the Serravallian about 13 Ma ago, leading to the partial drowning of the carbonate platform and the creation of shallow seaways. The initial bank-enclosed topography resembles an "empty bucket" geometry which is rapidly filled by the drift sediments that aggrade and prograde into the basin. Thereby the depositional environment of the delta drifts changes from deep water (> 500) to shallow-water conditions at their topsets, indicated by the overall coarsening upward trend in grain size and the presence of shallow water large benthic foraminifers at their top.

1. Introduction

Current-controlled carbonate deposits have so far not been systematically investigated in contrast to their intensively studied siliciclastic counterparts (Faugères et al., 1999; Stow et al., 2002b; Viana and Rebesco, 2007; Rebesco and Camerlenghi, 2008; Rebesco et al., 2014). Several studies, however, document their importance, especially in tropical carbonate platforms (Anselmetti et al., 2000; Betzler et al., 2009, 2013, 2014; Isern et al., 2004; Eberli et al., 2010; Lüdmann et al., 2012, 2013). For the Maldives, Lüdmann et al. (2013) demonstrated that since the Middle Miocene carbonate sedimentation in the Inner Sea was dominated by ocean currents entering the archipelago interior via gateways between the atolls. This situation resulted in the deposition of 10 mega-drift sequences. This is in contrast to the standard sequence stratigraphic model that describes carbonate platform geometry and depositional setting as a response to relative sea-level changes (Schlager, 2005 and references therein). Recent studies show that sea-level-controlled highstand shedding plays an essential role in sediment supply; However, currents could be the main agent transporting carbonate debris from the platform top and distributing it to the surrounding margins (Betzler et al., 2013, 2014, 2015; Lüdmann et al., 2013).

The Maldives, a large N-S elongated isolated carbonate platform southwest of the southern tip of India, are situated on an approximately 900 km long and 100 to 125 km wide submarine ridge consisting of a double row of atolls enclosing a deep basin, the Inner Sea (Fig. 1). It can be considered as a type locality for calcareous drift deposits. Here, in the deep water realm of the Inner Sea giant elongated drift bodies formed with geometric and seismic characteristics comparable to their siliciclastic counter parts with a typical mounded geometry and an associated moat (Lüdmann et al., 2013). Based on geometries depicted in reflection seismic profiles, we identified a new calcareous drift type at the mouth of the gateways. These drifts have a lobe-shaped external geometry with a clinoformal, prograding internal reflection configuration. We named the new sediment drifts delta drifts because they have much in common with river or tidal deltas. In 2015, during IODP Expedition 359 two platform-to-basin transects were drilled north and south of Goidhoo Atoll as well as in the Inner Sea (Betzler et al., 2016a, 2017, 2018). The cores and well logs through the delta drift deposits provide the sedimentological and stratigraphic data for the comprehensive analysis of the new drift type that is presented here (Fig. 1). This research presents new diagnostic criteria that allow the classification of carbonate sediment drifts and provide the base for further detailed studies of its sedimentological characteristics and facies associations. Results from this research will also potentially provide depositional models that could lead to a re-evaluation of carbonate deposits elsewhere and in the geological record that meet the new diagnostic criteria.

2. Geological background

The Maldives carbonate platform rests on a 55–57 Myrs old volcanic ridge. The Inner Sea basin, which is 300 to 350 m deep on average, is underlain by a fault-controlled en-echelon graben system (Purdy and Bertram, 1993; Aubert and Droxler, 1996) (Fig. 1). Reconstruction of the long term evolution of the Maldives was based on seismic data and industrial wells NMA-1 and ARI-1 from Elf Aquitaine and Shell as well as scientific drillholes of ODP leg 115 (Backman et al., 1988; Aubert and Droxler, 1992, 1996; Purdy and Bertram, 1993; Belopolsky and Droxler, 2003, 2004), and on the M74/4 cruise data (Betzler et al.,

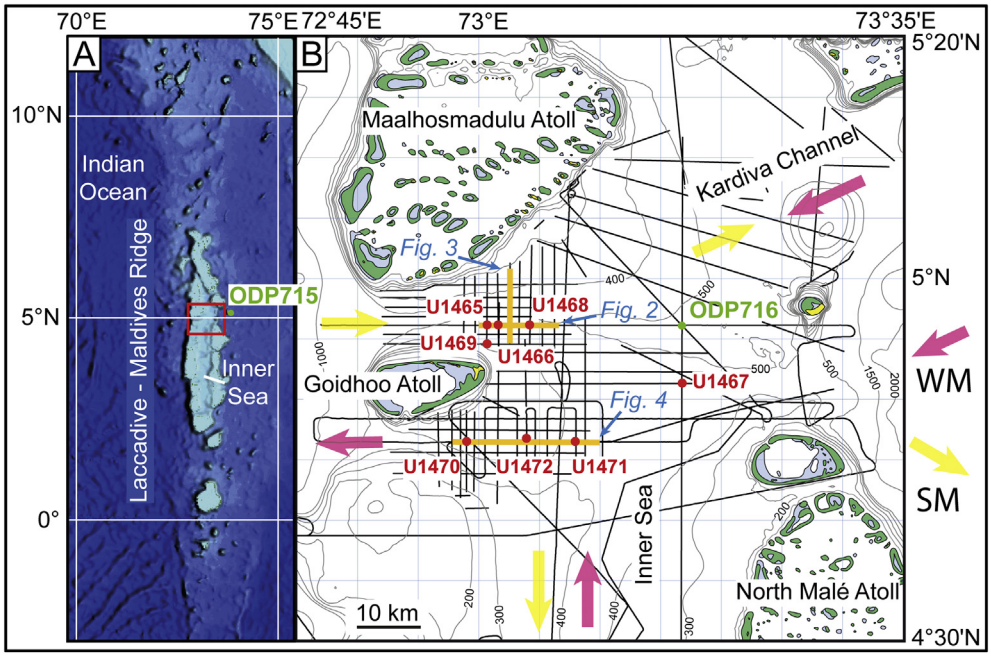

Fig. 1. A) Map of the study area (red box) in the northern part of the Maldives. B) Distribution of seismic lines (black lines) and the location of IODP Expedition 359 Sites as well as ODP Site 716 and 715. Indicated is the general present bottom current pattern below a water depth of about 200 m (compiled after Lüdmann et al., 2013). Example seismic profiles are marked in orange. Present reefs are color-coded (yellow: island; blue: reef; green: 10–100 fathoms). WM: winter monsoon; SW: summer monsoon. (For interpretation of the references to color in this figure legend, the reader is referred to the web version of this article.)

2009, 2014; Lüdmann et al., 2013). Subsidence was generally low averaging about 0.15 mm yr^{-1} to 0.045 mm yr^{-1} based on Pleistocene grainstones of Rashdoo Atoll (Gischler et al., 2008) and calculated from basalt depth of ODP Site 715 (Backman et al., 1988) located at the eastern margin of the Maldives (Fig. 1).

The Maldives are an isolated platform system far from any siliciclastic source assembling an almost complete Cenozoic sedimentary succession of exclusively calcareous material (Aubert and Droxler, 1992; Purdy and Bertram, 1993; Backman et al., 1988), with minor amount of aeolian dust (Betzler et al., 2016b). Sedimentation started with lacustrine deposits filling Eocene grabens accumulating sedimentary rocks in an anoxic environment (Aubert and Droxler, 1996). Eocene relative sea-level rise provoked neritic carbonate bank growth on the shoulders of the graben structures. A rimmed platform with a protected lagoon developed during the Early to Late Oligocene transition. In the Early Miocene (21.5 Ma) banks aggraded and prograded and a large central basin (the palaeo-Inner Sea) developed, surrounded by a narrow peripheral reef complex that faces the Indian Ocean (Aubert and Droxler, 1992, 1996; Betzler et al., 2009, 2012, 2016b). Seismic data show that the palaeo-Inner Sea was connected via the NE-Kardiva Channel (Fig. 1) with the Indian Ocean since the Middle Miocene (Aubert and Droxler, 1996; Lüdmann et al., 2013). Bottom currents could enter the semi-enclosed basin from the NE and flow along its western flank (Lüdmann et al., 2013). Aggradation of the platform margin continued into the Middle Miocene forming an “empty bucket” geometry of the palaeo-Maldives. During the late Early Miocene (18.15 Ma), the flat-topped carbonate bank margins started outbuilding towards the central part, thus beginning to narrow the size of the “empty bucket” (Betzler et al., 2016b). At the end of the Middle Miocene, the sea-level controlled depositional regime abruptly changed to a predominately current dominated system. This significant transition occurred about 13.0 Ma ago and is attributed to the onset and/or intensification of the Indian monsoon (Betzler et al., 2009, 2012, 2016b). This change to a current dominated system resulted in partial bank

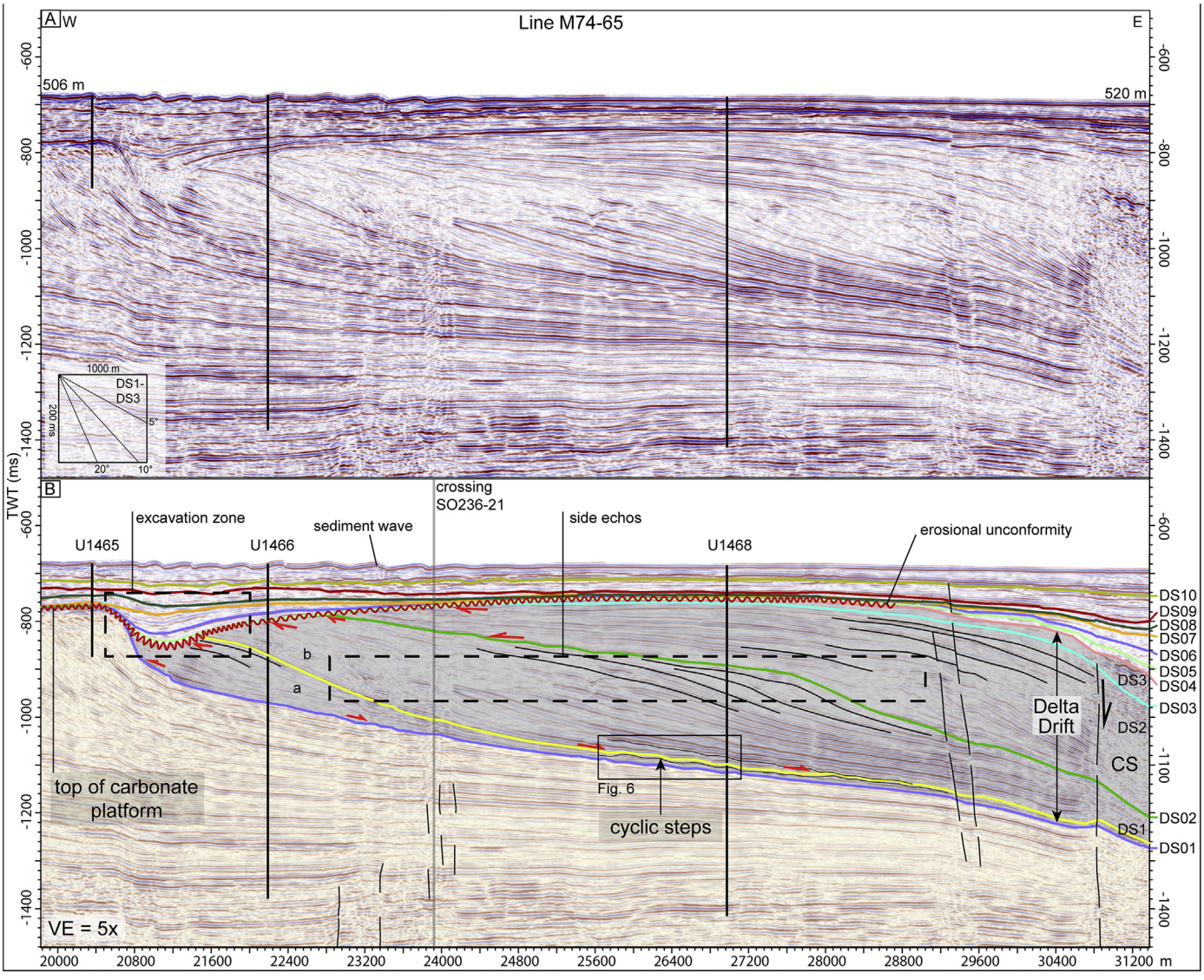

Fig. 2. A) Part of reflection W-E seismic line M74-65 that crosses the top of the Middle Miocene carbonate platform and delta drift north of Goidhoo Atoll in dip direction (for location see Fig. 1). B) Interpreted version showing mapped boundaries of the drift mega-sequences. Drift sequence DS1 can be subdivided into subsequence a and b. Indicated are the positions of the IODP Expedition 359 drillsites. Indicated in grey is the delta drift which rests on the exponential clinoforms of the former platform margin. Red wavy line marks a local erosional unconformity. Dashed lines exhibit possible fault traces. Red arrows show reflector termination. Black boxes reveal to an area of side echoes (see also cross line in Fig. 3) and an excavation zone (see text for further explanation). CS: collapse structure. Dip indicator: average velocity applied 1600 m/s. (For interpretation of the references to color in this figure legend, the reader is referred to the web version of this article.)

drowning of the platform margin, leading to the opening of passages that connect the Inner Sea with the Indian Ocean. Since then, 10 mega-drift sequences were deposited in the Inner Sea (Lüdmann et al., 2013; Betzler et al., 2017). Contemporaneously, the remaining atolls switched from a prograding to an aggrading mode (Betzler et al., 2009, 2016c). Drift sedimentation initiated in the northern part of the Inner Sea with the deposition of lobe-shaped drift bodies at the mouth of the gateways adjacent to the Goidhoo Atoll (Fig. 1). The northern gateway has a present width of ca. 12 km and a length of ca. 17 km as well as a swell depth of 510 m. The dimension of the southern one is almost the same but with 420 m it is shallower. At 5.8 Myr ago, when the depocenter migrated eastward, large elongated mounded drifts developed with associated moats along the eastern basin flank (Lüdmann et al., 2013). The latter is related to a northward flowing bottom current that entered the Maldives from the south. Recent studies demonstrate that the shallow water inner atoll environment likewise is current dominated (Betzler et al., 2015).

Present information on the oceanographic setting of the Maldives is rare (Knox, 1976). Fig. 1 shows the general bottom current pattern based on our cruises M74 (winter monsoon) and SO236 (summer monsoon) in the northern part of the archipelago (Lüdmann et al., 2013). During the summer monsoon, prevailing wind direction is towards east. Bottom currents (below 150 m water depth) enter the Inner Sea from the western gateways and exiting the Maldives to the east. In the central Inner Sea a southward flow dominates. The situation turns back during the winter monsoon, then bottom water masses entering the Inner Sea from NE and leaving it though the western gateways. The central Inner Sea is marked by a northward flow. This hydrodynamic pattern is overprinted by tidal currents that act especially in the narrow gateways and shallow channels of the atolls (Kench et al., 2009).

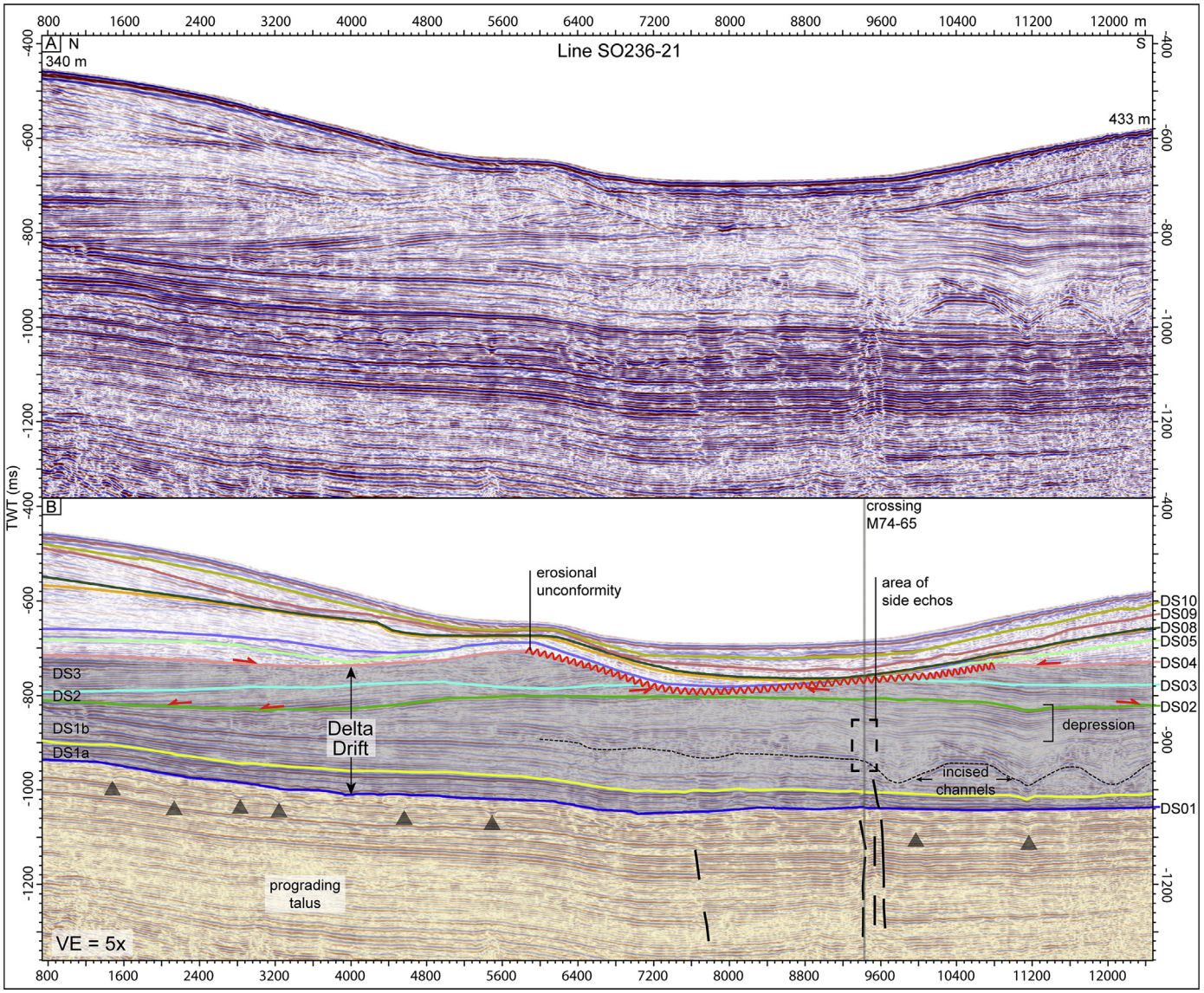

Fig. 3. A) Part of reflection N-S seismic line SO-236-21 that crosses the former platform talus and delta drift north of Goidhoo Atoll in strike direction (for location see Fig. 1). B) Interpreted version showing mapped boundaries of the drift mega-sequences. Drift sequence DS1 can be subdivided into subsequence a and b. Displayed in grey are the mounted delta drift lobe strata in strike view, underlain by the former platform foresets. Dotted black line indicates base of incised channel that are crossed perpendicular to their downdip trend. Red wavy line marks a local erosional unconformity. Black triangles point to the location of gullies that occur exclusively in the platform sequences and are absent in the drift sequences. Red arrows show reflector termination. Dashed black lines exhibit possible fault traces. Black boxes indicate an area of side echoes (see also cross line in Fig. 2 and text for further explanation). (For interpretation of the references to color in this figure legend, the reader is referred to the web version of this article.)

3. Data set and methods

The seismic data based on industrial and two multidisciplinary scientific cruises in 2007 and 2014, respectively. During these cruises a 144-channel digital streamer system with an active length of 600 m was used. Details about data acquisition and processing can be found in the initial IODP report Expedition 359 (Betzler et al., 2016a) and an earlier work by Lüdmann et al. (2013). IODP Expedition 359 was aimed to reconstruct the palaeoceanographic evolution of the Maldives over the past 23 Myr. To achieve the scientific goals, eight sites were drilled (U1465-U1472), aligned along two transects covering shallow to deep-water deposits (Fig. 1). The standard coring systems, the advanced piston corer (APC), extended core barrel (XCB), and rotary core barrel (RCB) were used. The APC was utilized in the upper portion of each site to obtain higher quality cores, with the exception of the platform top Site U1469 where only the RCB system was applied. Total penetration for the entire expedition was about 8725 m with the deepest drilled single hole reaching 1003.7 m below seafloor (Hole U1471E). However, due to lithification of the carbonates in the deeper sections at each site, total recovery was < 50% (3096 m). Downhole wireline logging was successfully performed at 4 sites (U1466 toU1468 and U1471). For the characterization of the sediment drift the lithostratigraphy, biostratigraphy, downhole logs as well as the physical properties of the IODP Leg 359 cores were used. A detailed description of methods can be found in the IODP Expedition 359 reports (Betzler et al., 2016a, 2017).

For time/depth conversion of the mapped sequence boundaries previous velocity models (Lüdmann et al., 2013) were fine-tuned by using the VSI velocity data acquired during IODP Expedition 359. Additionally, core lithology was correlated with the seismic facies and major lithological boundaries were tied to the mapped seismic unconformities (Betzler et al., 2018). By the use of post-cruise data some of the drift sequences ages were slightly corrected. Seismic-core-log correlation was carried out with the interpretation software package Petrel (Schlumberger). The 3D sequence surfaces are calculated in Petrel from the picked horizons using the convergent interpolation algorithm and a 100 × 100 m grid size.

4. Seismic architecture and facies

Seismic line M74-65 that runs through the western Kardiva Channel into the Inner Sea basin delineating a high-resolution cross-sectional view of the platform margin displays an apparent change in the geometry of prograding clinoforms (Fig. 2). The older clinoforms (marked as carbonate platform in Fig. 2) have horizontal topsets and steep concave foresets that are part of a prograding shallow-water platform. These concave clinoforms are onlapped by a large prograding sediment body with convex upward clinoforms, the delta drift (delineated as delta drift in Fig. 2). This abrupt change of geometry marks the transition from sea-level controlled platform progradation to current-controlled drift deposition at ca. 13 Ma ago (Betzler et al., 2016b). The delta drift in front of the channel north of the Goidhoo Atoll has a slightly mounded geometry in which the apex of the mound (located at the position of Site U1468, Fig. 2) is higher than the top of the former prograding platform despite being partially eroded (Site U1466; Fig. 2).

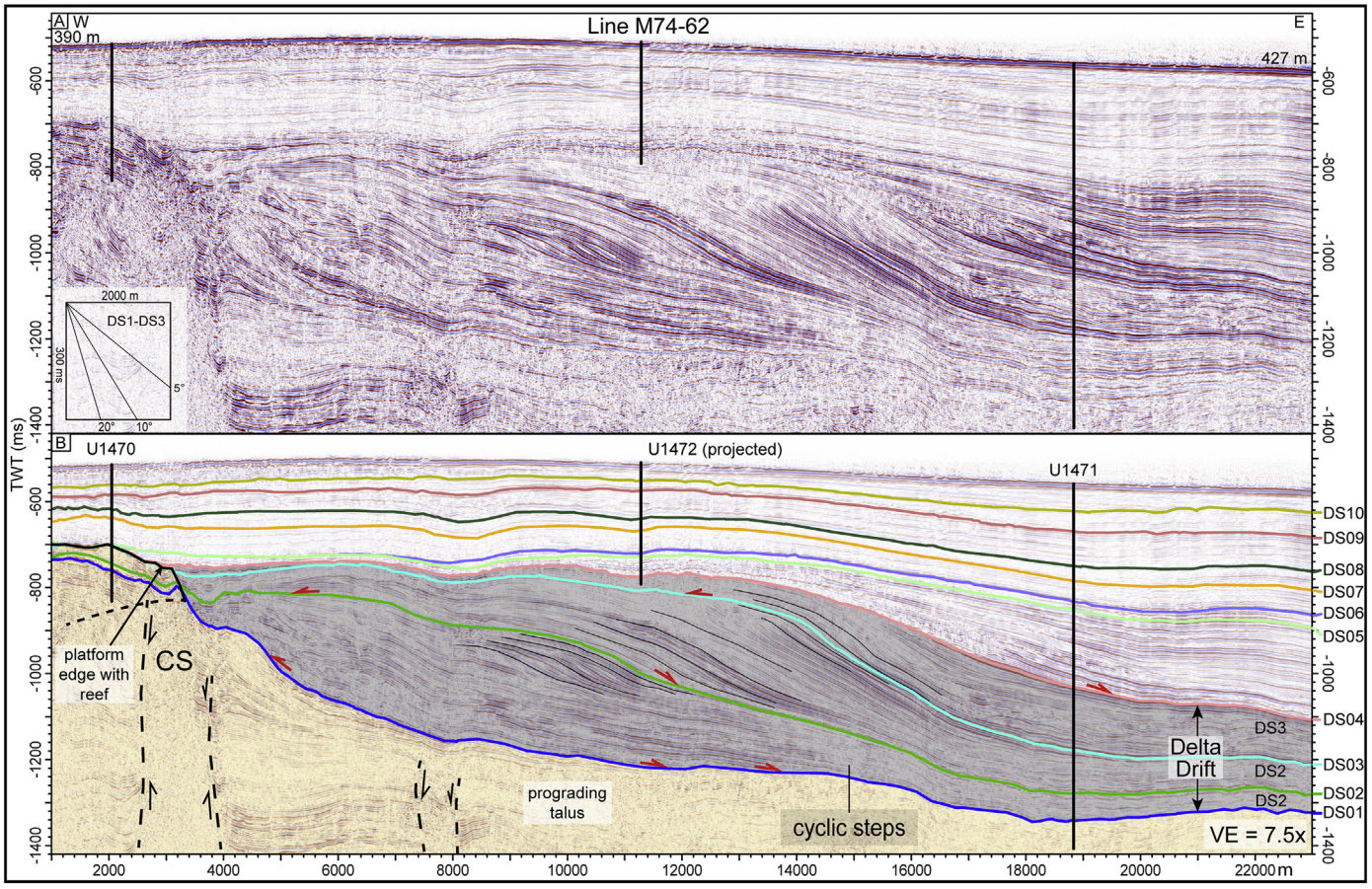

Fig. 4. A) Part of reflection W-E seismic line M74-62 that crosses the top of the Middle Miocene carbonate platform and delta drift south of Goidhoo Atoll in dip direction (for location see Fig. 1). B) Interpreted version showing mapped boundaries of the drift mega-sequences. DS1 is underlain by the prograding platform foresets, above in grey the sigmoidal clinoforms of the delta drift lobe. Marked with black lines are the clinoform roll-overs. Red arrows show reflector termination. Dashed black lines exhibit possible fault traces. CS: collapse structure. Dip indicator: average velocity applied 1600 m/s. (For interpretation of the references to color in this figure legend, the reader is referred to the web version of this article.)

Seismic line SO236-21 that is perpendicular to the dip of the delta drift displays channels carved into the prograding clinoform bodies (Fig. 3). Additionally, seismic line SO-236-21 shows the typical bi-directional downlap pattern of a lobe and its mounded across-strike geometry. A second prograding delta drift body, with similar geometries and seismic facies occurs in front of the channel south of Goidhoo Atoll (Fig. 4). The stacked lobes can be subdivided into three seismic mega-drift sequences (DS1–DS3) separated by major angular unconformities, characterized by onlap and downlap terminations (Figs. 2–4, red arrows). Basinward, the unconformities pass over into correlative conformities. North of Goidhoo Atoll mega-sequence DS1 can be further divided into two larger subsequences DS1a and DS1b. The seismic sections perpendicular to the depositional strike of the lobes (Figs. 2 and 4) display the nearly sigmoidal external shape of the sequences (DS1–DS3). They are characterized by gently dipping upper and lower segments and a thicker, more steeply inclined middle segment of prograding foresets. The upper segment shows a divergent reflection pattern with dip angles of 1°–3°. The thicker middle segment has foresets dipping basinward with angles of 3°–5°. The transition zone between the upper and middle segments is indicated by a continuous steepening of the slope forming a convex break-in-slope morphology (Figs. 2B and 4B, black curved lines). The lower segment is characterized by basinward thinning bottomsets that exhibit real or apparent downlap termination when their thickness falls below seismic resolution. Commonly the reflections indicate that strata are parallel and concordant with the sequence boundaries. Seismic line M74-62 south of Goidhoo Atoll runs southward of the deepest channel bed (Fig. 4). Here, the sequences DS1 to DS3 apparently pass over into the reef at the platform edge which was drowned at a later stage in the Tortonian compared to the northern channel. However, according to margin collapse the reflector transition from the edge to the slope strata is obscured and cannot be accurately determined (CS; Fig. 4). Most of the sediment was probably supplied from the immediately adjacent channel to the north that has cut into the platform top.

North of Goidhoo Atoll, the delta drift is marked in cross section by a depression like incision at the contact to the drowned Middle Miocene platform edge (Fig. 2). Here, parts of DS1 to DS3 are eroded and the depression is unconformably filled with younger sediments. At Site U1466, the hiatus spans ca. 6 Mill. yrs (Middle Miocene to Pliocene time) (Fig. 5). The channel axial profiles (Fig. 1) allow its spatial reconstruction which forms a local elliptical incision elongated along the drowned platform edge at the mouth of the northern channel (E, Fig. 5). Its major and semi axis is about 6.5 and 1 km, respectively. The maximum incision depth of 60 m is reached at profile M74-65 (Fig. 2).

Another specific feature seen in downdip view of the delta drifts is horizontal to down-cutting reflections that interrupt the uniform clinoform geometry as demonstrated in profile M74-65 (dashed black box; Fig. 2). In cross sectional view, this zone is the rim of a dip-parallel channel cut deeply into the foreset strata (dashed black box; Fig. 3). The southward dipping channel layers that are cut along strike create side echos and generate pseudo-horizontal down-stepping reflections. These dip-parallel channels in the drift sequences DS1 and DS2 cut at their base into underlying deposits, which is of particular importance. The channels are concentrated in DS1b, reaching varied widths of 500 m to 1 km and depths of 10s of meters to 150 m (Fig. 3). The channels depict linear conduits that are restricted to the steeper middle segment of the drift clinoforms and fading out basinward. There are no deep-sea fans attached to the mouth of these channels. After initial incision, the channels exhibit a divergent, aggradational infill pattern while the channel axis remains in the center. Laterally, the channel infill passes over into the layering of the drift sequences that form the delta drift, while the channel represents a local depocenter. In places, the channel can be traced as a smooth depression in the overlying foresets strata (depression; Fig. 3). In contrast to the aforementioned channels the platform sequences show a series of gullies (Fig. 3). They are considerably smaller in dimension reaching widths of only 100–300 m and depths of 10–15 m. Line SO236-21, oriented strike-parallel to the platform sequences displays a successive downward transition from proximal platform strata below DS1 to more distal strata. Here, the gullies are restricted and aligned along the most proximal strata representing the middle slope part of the platform clinoforms (Figs. 2 and 3). In general, our profiles depict that the gullies occur at the steeper upper to middle slope part.

At the base of DS1 wavy bottomsets appear near the toe-of-slope (Figs. 2 and 4). The waves have wavelengths of ca. 500 m and heights of 10–15 m. They have a distinct asymmetric shape and increasing wavelength in down-dip and in up-dip direction. A 3D image of their distribution demonstrates a slope-parallel N-S trend with the steep and shorter flank facing basinward (Fig. 6). Their stacking pattern indicates an upslope-migration (arrows; Fig. 6A).

The formation and early evolution of the delta drifts is depicted in Fig. 7. The computed surfaces of DS01 to DS04 illustrate their development of in front of the gateways north and south of the Goidhoo Atoll. Surface DS01 represents the antecedent depositional topography with a continuous platform to the west of the palaeo-Inner Sea, which

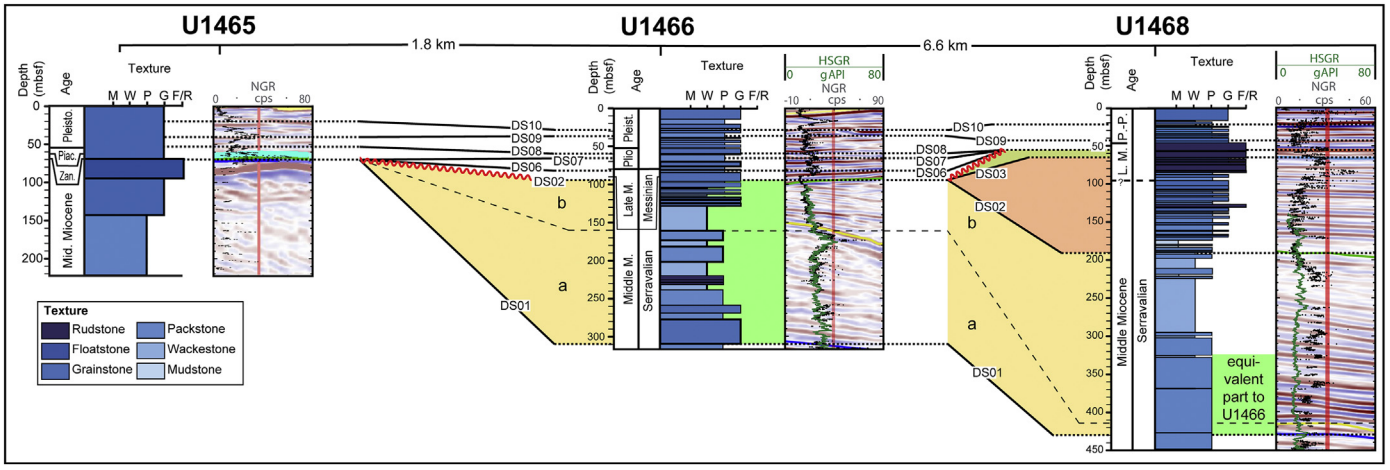

Fig. 5. Lithostratigraphic correlation of the IODP Expedition 359 Sites along the northern transect (see also Fig. 1). It crosses the platform top (U1465), the proximal upper slope (U1466) and the more distal middle slope (U1468) setting. Indicated are the boundaries of the drift sequences (DS). In color are DS1 to DS3, representing the deposits of the delta drift discussed in the text. Marked in green are the stratigraphically equivalent parts of DS1 and DS2 in Sites U1466 and U1468, respectively. In addition, core and log total gamma radiation are plotted with the seismic data (distance 250 m) at the well location (red line) in the background. Depth is shown in mbsf. (For interpretation of the references to color in this figure legend, the reader is referred to the web version of this article.)

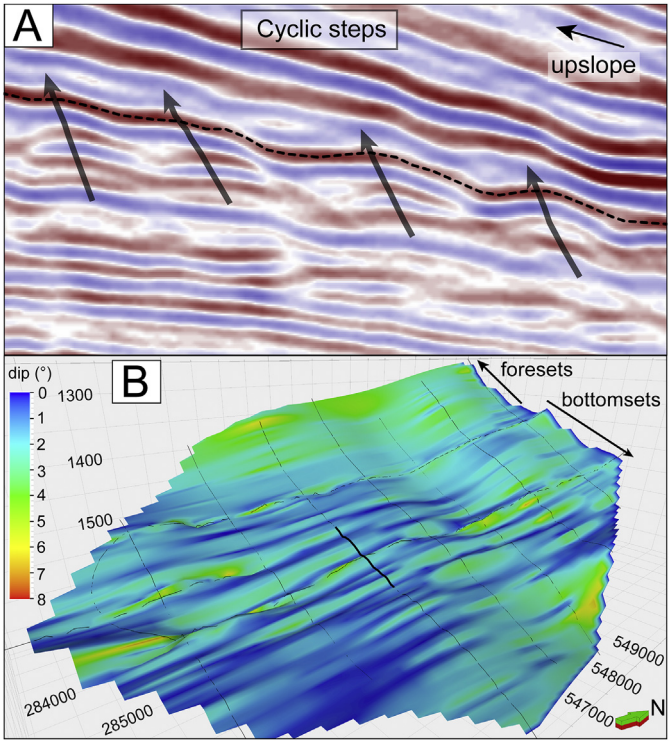

Fig. 6. A) Detail of profile M74-65 (see Fig. 2 for location) showing aggradational asymmetric cyclic steps with steeper basinward flank (transparent black arrows indicate upslope migration). B) 3D view of cyclic steps at the base of drift sequence DS1. Color-coded is the dip angle indicating a low upslope and a high downslope inclination of the margin-parallel sediment waves. It is characteristic for up-slope migrating asymmetrical cyclic steps after classification of Cartigny et al. (2011). (For interpretation of the references to color in this figure legend, the reader is referred to the web version of this article.)

was an approximately 500 m deep "empty bucket" surrounded by steep platform flanks (Fig. 7A). The onset of currents at about 13.0 Ma gradually carved channels into the carbonate platform. In the course of time these channels became deeper and wider (Fig. 7B–D). Compared to the southern channel, the northern one is much wider leading to the assumption that the effect of the bottom current was more pronounced in the north. Surfaces DS02 to DS04 (Fig. 7B–D) document the coeval progradation of the delta drifts into the Inner Sea and their successive deflection to the south. 3D geometry and cross sectional view of the delta drifts reveal their overall lobe-shaped morphology (Figs. 3 and 7). The lobes attained a maximal width of 16–17 km and a length of ca. 25 km, resulting in an area of 342 and 384 km^2, respectively. Their stratigraphic thickness reached up to 535 m and thereby filling the empty bucket in front of the channels.

The seismic facies of the delta drifts generally consists of continuous parallel reflections of low- to medium-amplitudes but in places, packages of strong reflections are observed (Figs. 2 and 4). These are particularly distinctive for the foresets of the southern delta drift clinoforms. Here, in the interval between 1000 and 1700 m very strong amplitude reflections occur in DS1–DS3 at the steepest part of their slope (Fig. 4). In contrast, the northern delta drift shows intervals of alternating medium to strong amplitude reflectors at the bottomsets of DS1 and the flat topped apex of DS2, between 26,000 and 30,800 m and 25,200 to 28,400 m, respectively (Fig. 2).

5. Lithology and age control

5.1. Sedimentation rates

The base of drift sequence DS1 at Sites U1466 and U1468 is dated to ca. 13.0 Ma, 11.7 Ma for DS2, to 10.55 Ma for DS3 and to 8.8 Ma for DS4 (Betzler et al., 2016b, 2017). In the thickest portions of the drift sequences, sedimentation rates lie around 17.0 cm ka^{-1} (DS1), 21.0 cm ka^{-1} (DS2) and 13.5 cm ka^{-1} (DS3). The entire delta drift was accumulated over 4.2 Myr with an average rate of 17 cm ka^{-1}. For the underlying platform sequences the sedimentation rate is significantly lower with about 4.4 cm ka^{-1} at the proximal location of Site U1466 and 3.2 cm ka^{-1} at the more distal location of Site U1468 (Betzler et al., 2016a).

5.2. Lithological content

Cores from Expedition 359 Sites U1466, U1468, U1471 and U1472 were drilled in order to characterize the facies of the drift sequences (Figs. 5 and 8A). Unfortunately, because of the deep incision at the former platform edge, large parts of the proximal deposits of DS1 and DS2 are missing in the northern transect, which makes the study of the downslope trends more difficult (Fig. 5). The delta drift deposits overlie the slope and basinal deposits of the drowned Middle Miocene platform. The platform sequences exhibit alternations of light (highstand) and dark, organic-rich (lowstand) layers (Fig. 9A). The lighter layers are thicker and formed by highstand shedding when the platform is flooded and most sediment is produced and exported, in contrast, the thinner darker layers are deposited during lowstand phases when the platform is exposed and sediment supply is reduced as is the case for similar deposits elsewhere (Droxler and Schlager, 1985; Schlager et al., 1994; Eberli et al., 1997). Bioturbation is common in the platform sequences and individual trace fossils can be discriminated. In contrast, the overlying drift strata are nearly uniform in color and a distinct lamination is absent. Bioturbation is detectable; however, the bioturbation degree is too high to identify individual burrows.

The lower part of the northern delta drift deposits (DS1a), consists of lithified, medium- to coarse-grained grainstone and packstone with abundant planktonic and benthic foraminifers, including minor large benthic foraminifers such as *Miogypsinoides* sp., *Lepidocyclina* sp., *Amphistegina* sp., and *Borelis* sp., together with other fragmented bioclasts in the proximal part, Site U1466. At the distal part, Site U1468, the lowermost facies of the delta drift consists exclusively of planktonic and small benthic foraminifers (Fig. 5). Bioturbation is very intense throughout, destroying the original texture. The vertical and lateral grain-size distribution for the northern delta drift shows coarser grained materials for the foresets of DS1a at Site U1466 (Fig. 10A) associated with a thin interval of finer bottomsets at Site U1468 (Figs. 2 and 5). With continuous progradation of the delta drift lobes, the deposits become finer at the proximal Site U1466 (Fig. 5).

At Site U1466, delta drift sequence DS1b is composed of medium- to coarse-grained, unlithified to partially lithified wackestone that gradually changes to packstone and grainstone towards the top of the sequence. The main components are small-sized benthic foraminifers, locally with some large specimen, planktonic foraminifers and minor bioclasts including red algae, bryozoans and *Halimeda* plates. Towards the top of the sequence, the facies changes into packstone and grainstone and large benthic foraminifera become the dominant component. This trend abruptly ends at the erosional unconformity with a sharp increase in planktonic foraminifers in the facies. In the more distal Site U1468, the sequence comprises packstone (Fig. 10A) that gradually changes upcore into wackestone (Fig. 10B). The main components are planktonic and small benthic foraminifers with rare sponge spicules. For DS1b, Site U1466 displays a coarsening upward trend; however, its top is eroded. Comparing the time equivalent strata of DS1b at Site U1468, the aforementioned trend of the topsets at the proximal Site is associated with no significant grain size variations of the bottomsets at the distal site. The facies of DS2 (missing at the proximal Site U1466) is composed of medium- to fine-grained packstones starting from the base of the sequence up to 178.5 mbsf at Site U1468. From this depth up to 150 mbsf, there is an overall coarsening-upward trend to a rudstone at

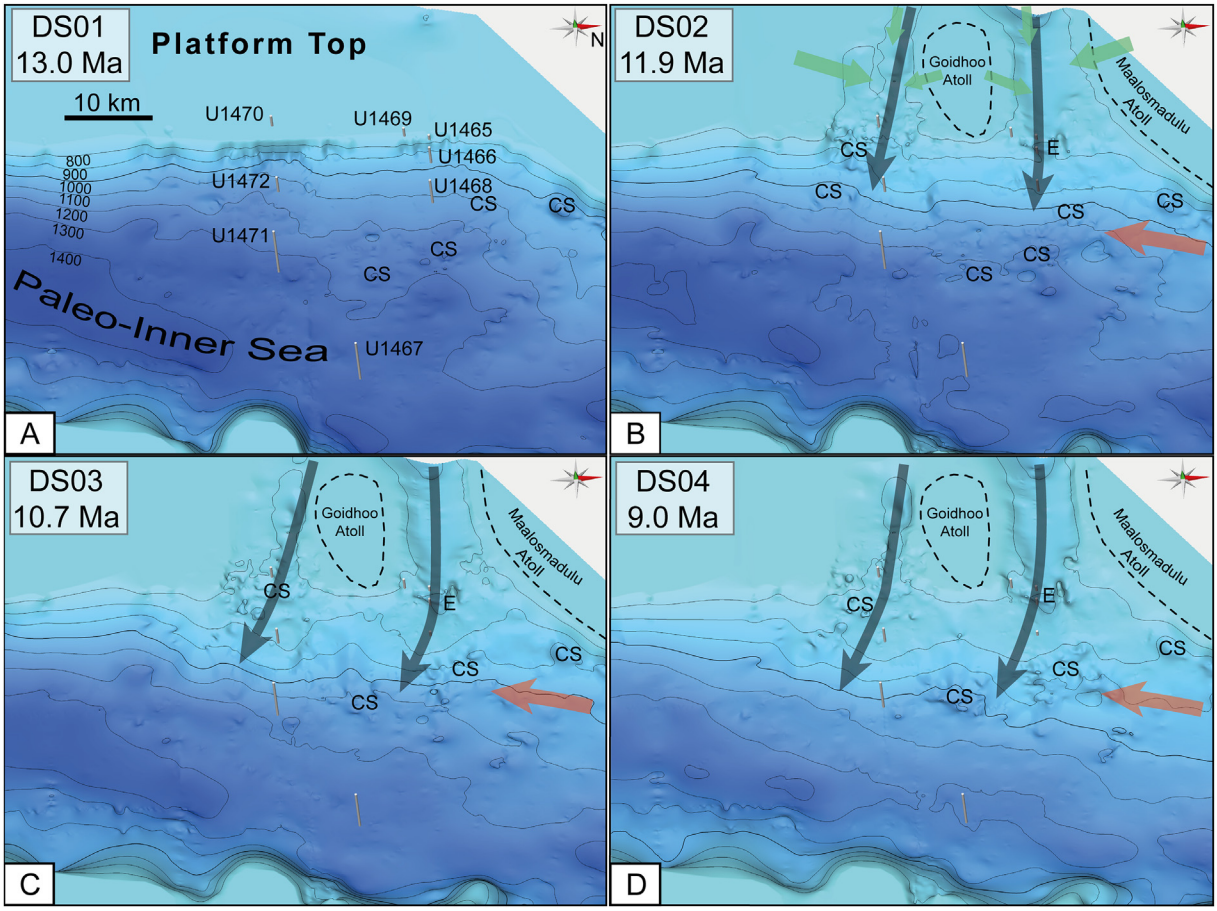

Fig. 7. Sketch of the Maldives palaeo-topography in the study area. View is to the west. A) Surface DS01 representing the initial "empty bucket" phase of the Inner Sea ca. 12.9 Ma ago. During this time the Inner Sea formed a semi-enclosed basin connected to the Indian Ocean via the northeast Kardiva Channel (Fig. 1). With the deposition of DS1 the platform top partially starts to drown and two proto-channels formed that connect the paleo-Inner Sea with the Indian Ocean. B) Top of delta drift sequence DS1 (DS02) demonstrating the lobe-shape infill of sequence DS1 attached to both waterways. The depocenter is deflected slightly southward by a south directed contour current (red arrow). Green arrows indicate possible sediment sources. C) Top of delta drift sequence DS2 (DS03) showing the progradation of sequence DS2 into the Inner Sea basin. DS2 continued to be deflected southward. Channel widening dominates over channel incision by platform backstepping. D) Top of delta drift sequence DS3 (DS04) revealing the final stage of delta drift formation ceasing at ca. 9.0 Ma. Indicated are the positions of the IODP Expedition 359 Sites. Isolines show depth in TWT. Red arrows indicate an assumed slope-parallel current, entering the Inner Sea from the deep eastern Kardiva Channel (see Fig. 1 for location). CS: collapse structure; E: excavation. (For interpretation of the references to color in this figure legend, the reader is referred to the web version of this article.)

the top of the sequence (Fig. 5). Locally, shorter intervals of coarsening-upward and fining-upward occur. The coarser intervals are rich in large benthic foraminifers (*Amphistegina* sp., *Lepidocyclina* sp., *Miogypsinoides* sp., *Heterostegina* sp., *Operculina* sp., and *Sphaerogypsina globulus*) and locally in echinoid spines, red algae, mollusk fragments, branching and encrusting bryozoans, *Halimeda* plates. Aggregated grains are also present (Fig. 10C and E). Planktonic foraminifers are absent in this sequence and the abundance of large benthic foraminifers increases upcore reaching a maximum at the top of the sequence. The facies of DS3 is similar to those from the top of DS2 with large benthic foraminifer-rich rudstones (Fig. 5). Bioturbation in sequences DS2 and DS3 is intense and single burrows are not identified. In the southern transect there was an active carbonate platform by the time of the initial delta drift deposition (Fig. 4). The platform sediments at Site U1470 (Fig. 8A) are coeval to the drift sequences DS1 to DS3 and consist of shallow water carbonates with abundant corals and coralline algae. Site U1471 (Fig. 8A), in a more distal position, displays a distinct facies for the delta drift sequences. Here, the facies in DS1 consists of alternating fine-grained planktonic foraminifer-rich packstone and grainstone. Planktonic foraminifers, calcareous bioclasts, and calcareous nannofossils are abundant, and benthic foraminifers are a minor component. Bioturbation is abundant to common. Grainstone intervals often have a sharp basal contact with the underlying packstone. The overlying sequence DS2 consists of very fine to fine-grained wackestone to packstone with abundant planktonic foraminifers, and common to present sponge spicules, radiolarians, and calcareous nannofossils. Delta drift sequence DS3 in its proximal position (Site U1472; Fig. 8A), comprises medium- to coarse-grained partially lithified planktonic foraminifer-rich grainstone and packstone. The main components are abundant planktonic foraminifers, benthic foraminifers, and aggregate grains/intraclasts. Among the large benthic foraminifers there are *Amphistegina*, *Lepidocyclina*, and *Miogypsina*. Mollusk fragments, gastropods, echinoid fragments, coral remains, as well as *Halimeda* and red algae fragments are present to rare. Basinwards, at Site U1471, DS3 facies changes into fully lithified very fine to coarse-grained planktonic foraminifer-rich wackestone to packstone that gradually evolve to packstone and grainstone, at the top of the sequence. Towards the top of the sequence benthic foraminifers and mollusk fragments are common.

5.3. Logs and physical properties

Figs. 5 and 8A show the core (NGR) and high-resolution downhole (HSGR) natural gamma radiation profiles. The total gamma radiation signal is dominated by the contribution of uranium, with only minor

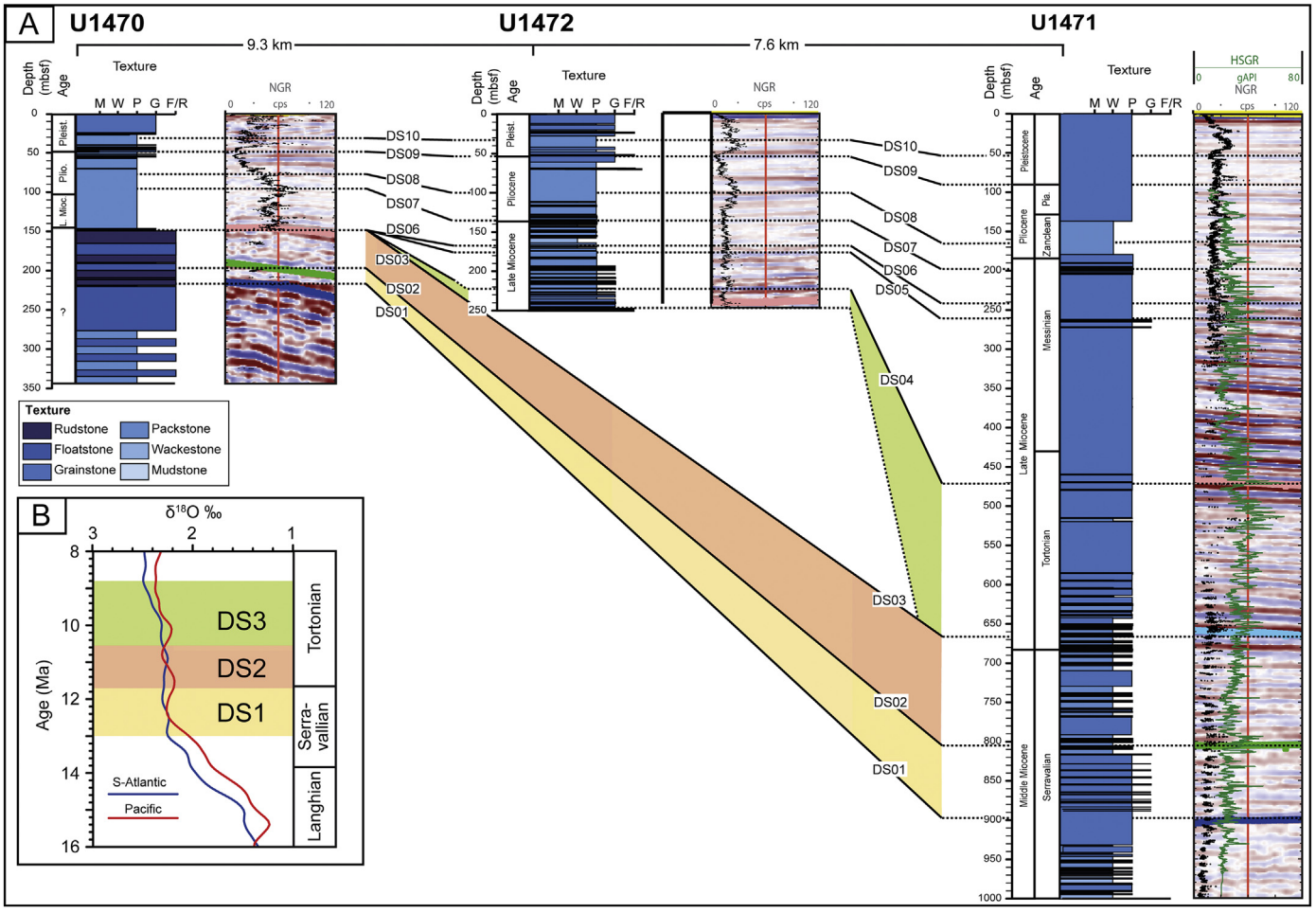

Fig. 8. A) Lithostratigraphic correlation of the IODP Expedition 359 Sites along the southern transect (see also Fig. 1). It crosses the platform top (U1470), the proximal upper slope (U1472) and the more distal middle slope (U1471) setting. Indicated are the boundaries of the drift sequences (DS). In color are DS1 to DS3, representing the deposits of the delta drift discussed in the text. In addition, core and log total gamma radiation are plotted with the seismic data (distance 250 m) at the well location (red line) in the background. Depth is shown in mbsf. B) $\delta^{18}O$ curve for the South Atlantic and Pacific after Cramer et al. (2011) with location of the delta drift sequences DS1 to DS3. (For interpretation of the references to color in this figure legend, the reader is referred to the web version of this article.)

contribution from thorium or potassium (Betzler et al., 2016a). Uranium variations most likely relate to the amount of organic matter. There is a clear discrepancy between NGR and HSGR at Site U1468 (Fig. 7) which may be explained by a closed caliper during downhole logging, leading to an inadequate borehole size correction of the HSGR. Here, the NGR measurements are more reliable. In general, the sequences DS1 to DS3 of the delta drift show a gamma radiation with a smoother overall trend but with a clear difference in the distal part of the northern and southern transect, respectively (U1468 and U1471; Figs. 7 and 8A). In the north the values are lower and show less variability. However, at both sites the sequence boundaries DS1–DS3 are marked by changes in radiation, especially at Site U1471. As a distinctive feature at Site U1468 there is a pronounced increase in NGR at the top of sequence DS2. Both NGR und HSGR data from Site U1468, as well as NGR data from Site U1466 (below the depth where logging data could be recorded), show a pronounced interval of increased organic matter content within the bottom sets of the platform sequences with a high variability of the gamma radiation.

Physical properties at the proximal Site U1466 exhibit a continuous increase in bulk density with depth to about 300 mbsf while porosity decreases (Fig. 9B). Below that depth density and porosity remain nearly constant. This trend is also expressed by the seismic facies, the less dense drift sequences exhibit much lower reflection amplitudes compared to the platform strata (Fig. 5). At distal Site U1468, there is an abrupt change at about 45 mbsf to nearly constant values below. This depth coincides with the unconformable contact between delta drift topset and overlying younger sheeted drift strata. The latter is characterized by low bulk density and high porosity, whereas, generally, the delta drift sequences DS1 to DS3 show a normal density and porosity trend with increasing burial depth.

6. Discussion

We classify the herein described lobe-shaped sedimentary bodies as drift deposits that mainly accumulated though the action of persistent bottom currents. We denominate these bodies delta drifts, they represent different features compared with contourite fans. The latter, originally described a siliciclastic fine grained fan-shaped body from the Vema Channel in the Brazilian basin, downstream of a deep-water gateway which was assigned it to abyssal plain contourites (Mézerais et al., 1993; Faugères et al., 2002; Hernández-Molina et al., 2008). Carter and McCave (1994) used the term fan drift attributed to a turbidite fan that extended into a drift. Locker and Laine (1992) introduced a companion system comprising a submarine fan/drift interaction. Such deposits, however, are different from the delta drifts we observed in the Maldives. Sensu stricto a contourite drift is defined as a sediment drift, principally formed by deep-water bottom currents (Stow et al., 2002a), however, the delta drifts observed in the Maldives are not related to deep water bottom currents. Additionally, the term contourite emphasizes current orientation with respect to the bathymetric

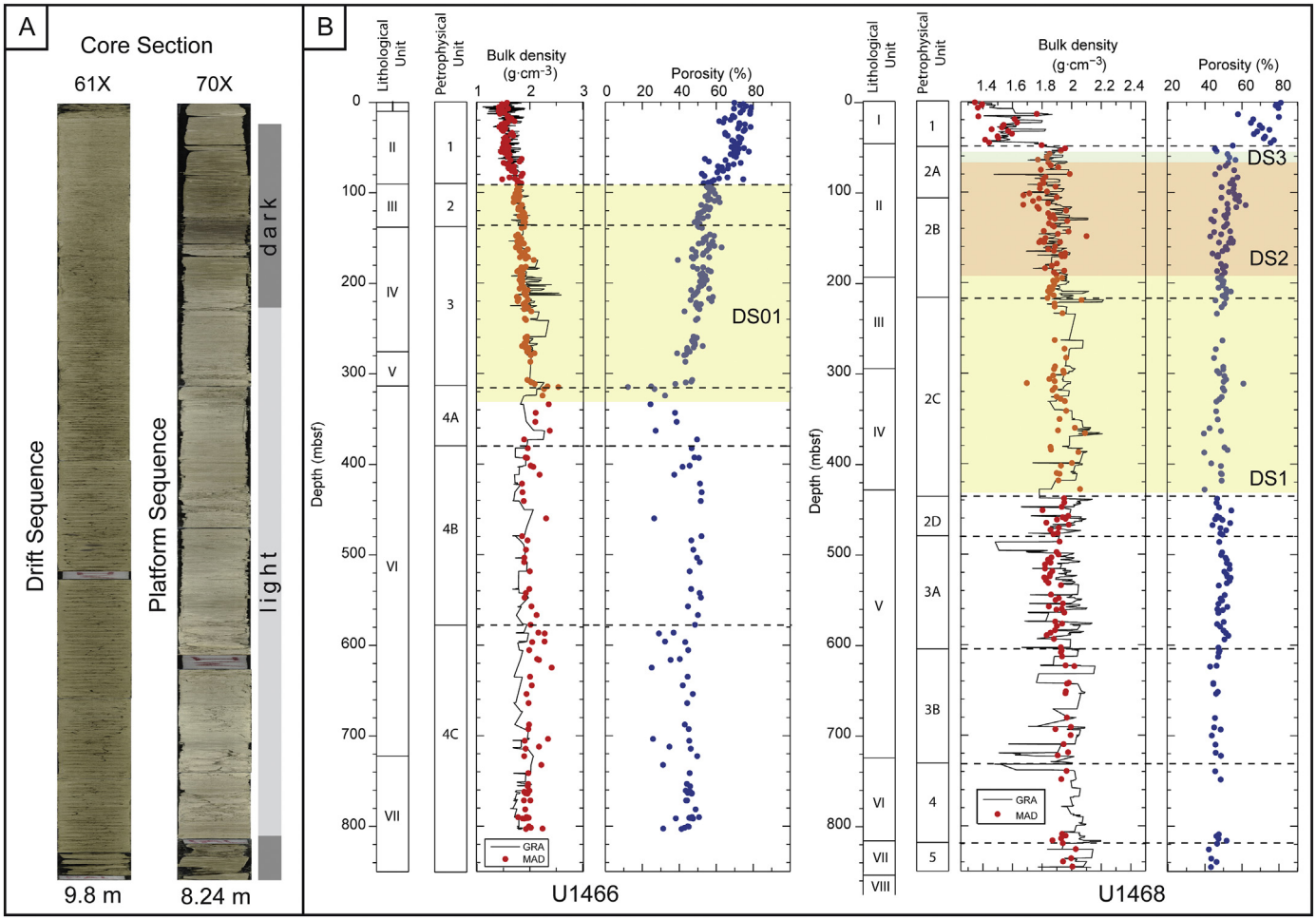

Fig. 9. A) Core section 61× (379.2 mbsf) and 70× (466.6 mbsf) of Site U1468 showing typical drift and platform slope strata, respectively (see Fig. 1 for location). Characteristic is the color change of the platform slope sequence. B) Bulk density and porosity measured on cores from Sites U1466 and U1468.

contours. The newly discovered delta drift is related to a relatively shallow water gateway and predominantly formed by currents that expand at the exit of the gateway and preferably run downslope as an underflow perpendicular to the isobaths. It can be best described as delta-like current-controlled deposits. The northern delta drift consist of four lobes and the southern one of three lobes resembling sequences DS1a, DS1b, DS2–DS3 and DS1–DS3, respectively.

6.1. Delta drift characteristics

There are several lines of evidence that indicate the current-controlled nature of the delta drifts. A compilation of their characteristics is found in Fig. 11. First a comparison of the clinoform architecture of the platform and the drift sequences (DS1–DS3) clearly underpin their differences, because they exhibit an obvious contrast in slope curvature: the sea-level driven platform clinoforms have a distinct concave shape created by the foresets whereas the drift sequences exhibit a convex upward geometry (Figs. 2, 4 and 11). The 3D image clearly documents that the lobe-shaped sedimentary bodies are connected to the basinward channel exits and so do not represent a sea-level controlled regression of the platform margin (Fig. 7). Furthermore, typical gravitational foreslope deposits like slumps or debris flows have not been identified in either core samples or the seismic data. In addition, gullies as we found in the platform sequences (Fig. 3) do not exist in the delta drift. The only indication for downslope gravity-induced mass transport is observed in the distal part of the drift at Site U1471. Here, convolute bedding and soft-sediment deformation occurs at the base of the wackestone interval in drift sequence DS1 (Fig. 8A). They might be products of sediment remobilization (Phillips, 2006). However, taken into account that no clear grading was identified in these layers and that some contacts were gradational at both, the base and top of the grainstone layers, it is more likely that these intervals represent high-current events related to the migration of bottom current.

Several observations argue for the action of long-lasting bottom currents and meet the criteria established by Stow and Faugères (2008) for the recognition of drift deposits. (1) The absent of bedding and lamination structures. In contrast to the gravity-controlled deposits of the platform sequences typical black and white layers or distinct laminations are lacking in the delta drift strata which are uniform in color. (2) Grain size from sand to clay. The grain size varies from coarse sand (e.g. large benthic foraminifers) to fine carbonate debris. (3) The degree of bioturbation. The latter is intensive and continuous (see results section). (4) Variable, low to moderate sedimentation rates. Cycles of normal and inverse grading point to a persistent bottom current flow with variation in mean current velocity or sediment supply. The latter was relatively high and the average sedimentation rate of 17 cm ka^{-1} of the delta drifts notably differs from the platform sequences with 4.4 to 3.2 cm ka^{-1}. It is comparable to rates on mounded drifts, assigned to 5–30 cm ka^{-1} by Stow et al. (2008). When accommodation space was filled and the top of the delta drifts reached the swell depth of the channels, current speed increased as indicated by the dominance of grain- and rudstones (Fig. 5, U1466 and U1468). This point to intensification in transport energy of the current leading to the re-deposition of larger components and the winnowing of the finer fraction.

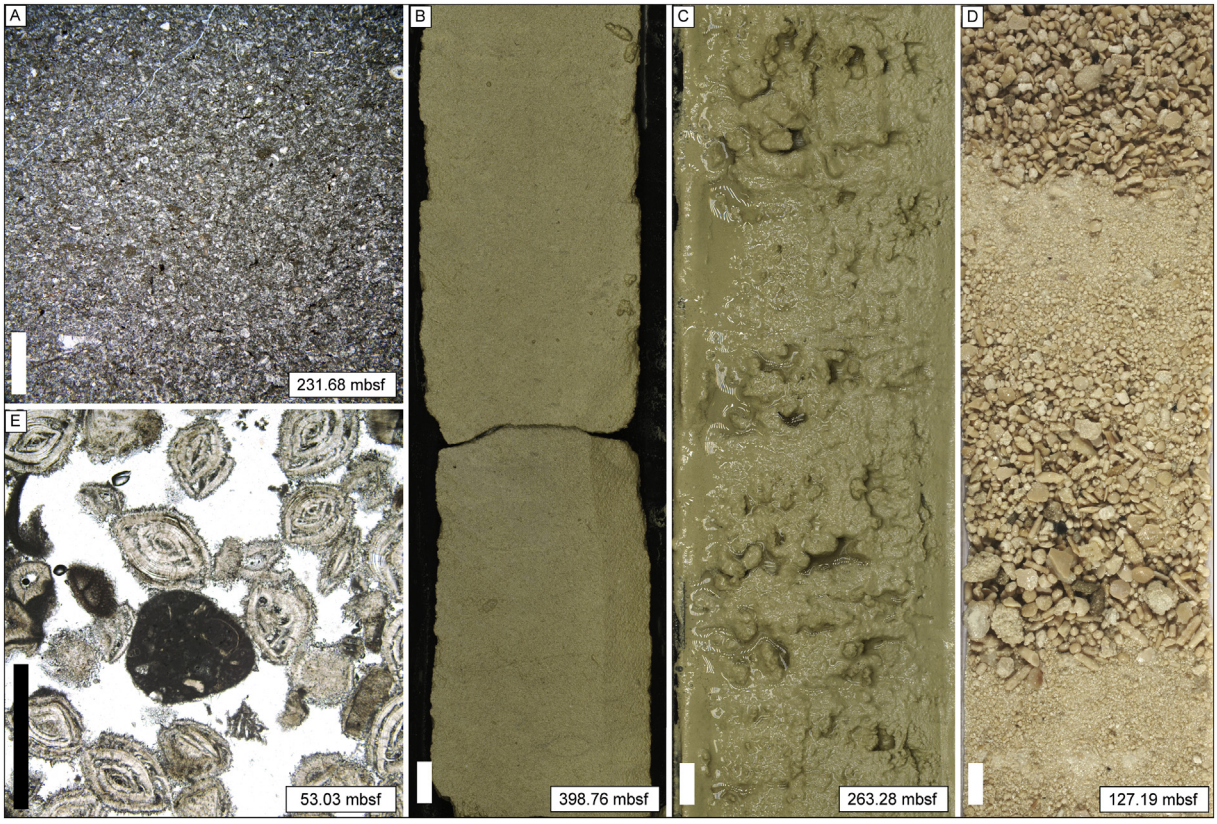

Fig. 10. Facies of the delta drift (scale bar for core photographs = 1 cm, scale bar for photomicrographs = 1 mm). A) Core photograph of a fine-grained bioclastic packstone at Site U1468. B) Core photograph of an unlithified wackestone with intraclasts at Site U1468. C) Core photograph of a large benthic foraminifera-rich rudstone to grainstone with fining upward at Site U1468. Echinoid spines and intraclasts are common. D) Photomicrograph of the fine-grained packstone at Site U1466. E) Photomicrograph of the rudstone to grainstone facies at U1468 with abundant Amphistegina and intraclasts. See also Fig. 5 for location of samples.

The filled accommodation space resulted in a shallowing of the environment as evidenced by the dominance and diversity of large benthic foraminifers and the occurrence of coralline algae and *Halimeda* plates.

In general, the delta drifts show a proximal to distal fining trend. Basinward, very fine to fine sand-sized carbonate grains dominate and grainstones are rare. The occurrence of grainstones could be related to winnowing of the fine fraction by the postulated slope-parallel current that slightly deflected the depositonal center of the delta drifts to the south (red arrow; Fig. 7B to C). However, this current played only a minor rule in the formation of the delta drifts.

The wavy bottomsets at the base of the delta drift are herein interpreted as cyclic steps, as described for similar up-slope migrating down-slope asymmetrical sedimentary structures (Cartigny et al., 2011). The cyclic steps near the toe-of-slope are typical for the early stage of delta drift development, when the slope profile is steeper (Figs. 2 and 4). In their up-section they fade out, most likely related to a change in hydraulic regime associated with successive reduction in slope curvature. Unfortunately, the recovery in DS1a at Site U1468 is very low and details of the sedimentary facies of the cyclic steps cannot be determined. Principally, they represent a lithified packstone interval with no significant differences to the overlying strata.

Another specific feature of the delta drift are channel-like features that cut into the lobe surface down-current from the lobe apex (Fig. 3). They might be an indication for a multicore bottom current with individual flows (Fig. 11). The current remained stationary along these incised tracks while sedimentation continued over the entire lobe. Contemporaneously, the current channels were filled above the incision level and prevailed as depressions where the current stayed active (Fig. 3). The depositional elements of the mapped delta drift slope channels are not comparable to siliciclastic deep water channels or slope valleys as described for example by Deptuck et al. (2007), McHargue et al. (2011), Janocko et al. (2013). These include high-amplitude reflection patches, lateral accretion packages, onlap fill patterns and channel-levee-overbank complexes.

Giant excavation structures in the topsets of the delta drift lobes like the oval-shaped depression at the contact to the northern channel mouth represent another distinctive feature. Here, the loosely packed, non-cohesive delta drift strata onlap the former cemented platform edge (Fig. 2) and a bottom current intensification may have been responsible for the excavation. When the confined and accelerated bottom current that exits the channel reaches a threshold velocity it may generate a turbulent flow at the lithological contact, eroding into the unconsolidated delta drift beds by sweeping away the sand-sized carbonates. When this process lasted for longer periods it created the observed large oval-shaped depression in front of the platform edge that was later refilled by younger sediments (Figs. 2 and 7b–D). According to the bio-stratigraphy of Site U1466 the excavations formed after the deposition of delta drift sequences DS1 to DS3 (Fig. 5).

6.2. Depositional environment

Prerequisites for a delta drift development are: a persistent sediment supply from a point source and sufficient available accommodation space. Suitable point sources in carbonate platform setting are inter-atoll gateways that connect the open ocean with the platform interior shedding huge volumes of material from different source areas into a receiving basin. The water masses flowing through the channels catch up fallout from the water column of dominantly planktonic microfossil assemblages from the Indian Ocean side as well as calcareous debris driven from the adjacent atolls and produced by the organisms living in the gateways (Fig. 7B, green arrows). An additional source are benthic organisms including large foraminifers colonized the flatted top of the

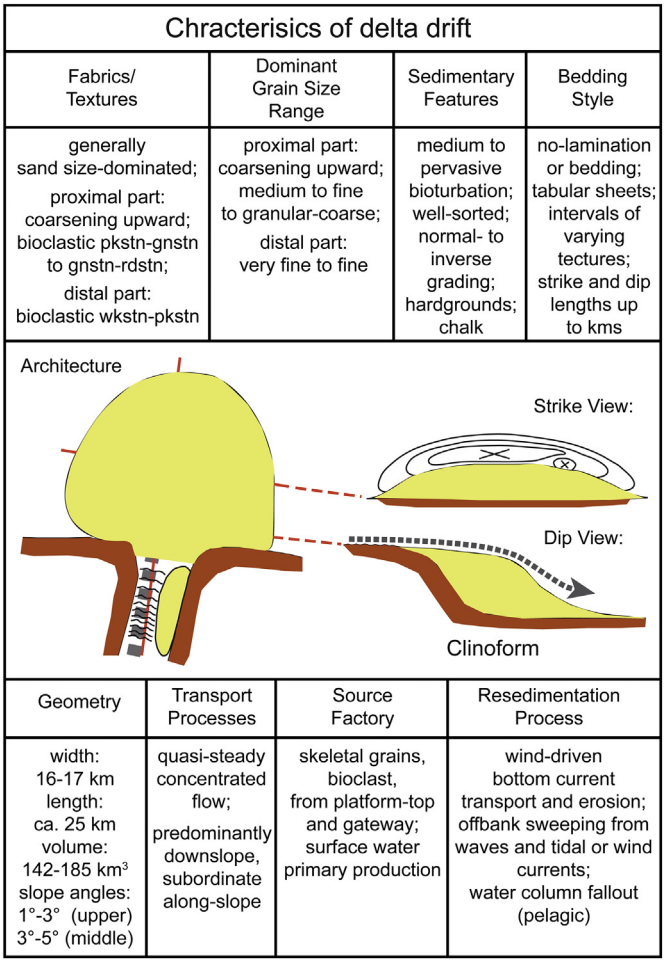

Fig. 11. Summary of the delta drift characteristics, including a sketch showing the channel-related drift in strike and dip view. Gnstn: grainstone; pkstn: packstone; rdstn: rudstone; wkstn: wakestone.

delta drift and planktic organisms living in the water column above the drift. Erosion of the former drowned platform top played only a minor role in the sediment budget. We calculate the total volume of the northern delta drift to be 142 km^3 and the redeposited material eroded from the channel base accounts for only 0.05%. On the western side of the archipelago, the west-east flowing current driven by summer monsoon winds is stronger and the dominant driver pushing Indian Ocean water masses into the Inner Sea (Purdy and Bertram, 1993; Storz and Gischler, 2011). This dominant current direction explains the distinct lobe-shaped morphology at the exit of the two gateways. Changes in the flow regime possibly triggered by major oceanographic or climatic alternations have result in the formation of major unconformities separating the delta drift sequences DS1–DS3.

In the case of the Maldives, these gateways formed by partial drowning of the surrounding platform top in the late Middle Miocene ca. 13 Ma ago and were initiated by a modification in water mass circulation induced by the beginning of monsoon intensification (Betzler et al., 2009, 2016b). Smaller inlets are still common for the modern Maldives atolls implying that the reef rim facing the ocean is generally not a closed feature. The mechanism behind the transformation of these inlets into large gateways remains speculative and needs further research. Compared to the small inlets, the gateways allow the exchange of large volume of water between the surrounding ocean.

Accommodation changes related to relative sea-level may have played only a minor role in the formation the delta drifts. Fig. 8B documents that the drift sequences DS1–DS3 were deposited during a phase of minor sea-level fluctuations as shown by benthic foraminiferal $\delta^{18}O$ values for the Atlantic and Pacific (Cramer et al., 2011). Coevally, there was no substantial influence on sea-level based on ocean basin dynamics (Müller et al., 2008). A rough estimation of the post-Middle Miocene subsidence rate provides a low value of 0.044 mm yr^{-1} that fits very well with the rate deduced from ODP Site 715 (see Geological background). For the calculation we used the top of the carbonate platform at the base of DS1 (13.0 Ma) at Site U1465 as a past sea-level indicator (Fig. 2). It lies at the present depth of ca. 570 mbsl. Because of its thin sedimentary cover consisting of loosely packed carbonate sand (Fig. 5; Site U1465) compaction is negligible. Palaeo-sea level was almost the same as today (Kominz et al., 2008). Coral reefs growing at rates of 10 mm yr^{-1} (Schlager, 2005) could easily catch up with the low subsidence rate.

Accommodation during the growth of the delta drifts was mainly controlled by the preexisting depositional topography of the Inner Sea and the magnitude of sediment supply. At the ocean facing margin of a carbonate platform a delta drifts cannot develop because accommodation space is generally too large; the slope profile generally rapidly declines to abyssal depth and sediment export outside the platform through the gateways is negligible. The delta drifts developed in a shallower basin with few hundred meters of water depth. The Maldives palaeo-Inner Sea with an approximate 500 m water depth fits in this category (Fig. 7A). The gateway delivering the sediments is not changing its base level, in fact the delta drift attached to the gateway exit aggrades up to this level and at the same time outbuilds into the interior basin filling the Inner Sea and eventually has a crest that is higher than the spill height of the channel (Fig. 2). The bottom current in the gateway provides a steady sediment supply and distributes the sediments after leaving the gateway along the slope profile, generating a Gaussian curvature and keeping the angle-of-repose below a threshold for triggering significant slope failure. Distinct changes in current speed occurred as documented by the waning and waxing structures of the sediments. They are possibly related to variations in monsoon wind strength as well as widening and/or deepening of the gateway induced by sea-level fluctuations. These variations in current speed could have also influenced the organic matter proportion in the delta drift sequences as indicated by the natural gamma radiation. Wetzel et al. (2008) proposed that higher current speeds generally winnow out organic matter. There is a slight trend in increasing gamma ray values at the top of each sequence, which in turn is related to a decrease in current speed. However, variations in nutrient supply is another important factor.

7. Conclusions

Reflection seismic data together with cores and logs from IODP Expedition 359 document a new sediment drift type located in front of two gateways. We term this new type a delta drift and classify it as a channel-related drift that is emplaced under a long-term, current-driven sediment flux regime. Our data do not show indication of significant gravity-controlled sedimentation in the delta drift. The drift bodies form stacks of individual lobes in front of two gateways. Both delta drifts are nearly identical and are deposited in front of the edge of a drowned carbonate platform. The main characteristic of the delta drifts discovered on Maldivian carbonate platform are:

- The delta drifts are situated in the Inner Sea basin at the downstream exit of a shallow and over time deepening gateway. In contrast to a fluvial delta system, the delta drifts accumulated considerably below base level;
- Individual lobes may built up stacks that resemble a delta drift;
- Current flow was wide-ranging on the drift body perpendicular to the isobaths. Smaller channels running downdip are developed on top of the delta drift lobes indicating that they must have been fed by a multicore current;
- The delta drifts exhibit progradation with pronounced sigmoidal

clinoform geometry. Their spatial extent is about 342–384 km^2 and the depositional relief reaches up to 500 m;
- The delta drifts show a distinct coarsening upward trend in grain size, related to a shallowing of the depositional setting when accommodation space is filled up to the level of the feeder channel bed;
- During the early phase of deposition, when the depositional profile of the slope was still concave from the underlying distal slope clinoforms, cyclic steps developed at the toe-of-slope;
- Large excavations with depths of up to 80 m may occur where the bottom current overflows beds of consolidated and unconsolidated material and turns into a turbulent flow. They reach dimension of 10 km^2 and preferably develop at the onlap termination of the former cemented platform edge and the loosely packed coarse delta drift topsets.

Acknowledgements

Our special thanks go to the IODP Expedition 359 drilling crew, ship's crew and scientific staff of the Drillship JOIDES Resolution. The expedition was funded by the US National Science Foundation (NSF); the European Consortium for Ocean Research Drilling (ECORD); the Ministry of Education, Culture, Sports, Science and Technology, Japan (MEXT); the Ministry of Science and Technology (People's Republic of China); the Korea Institute of Geoscience and Mineral Resources; the Australian Research Council and the New Zealand Institute for Geological and Nuclear Sciences; and the Ministry of Earth Sciences (India). The German Federal Ministry of Education and Research is thanked for funding the seismic surveys (03S0405, 03G0236A). Additional acknowledgements go to the companies HALLIBURTON-LANDMARK, SCHLUMBERGER and CEGAL Geosciences for providing university grants for the seismic processing software PROMAX and seismic interpretation software PETREL as well as its BLUEBACK plugin. We thank M. Rebesco, as the editor of this manuscript, and T. Mulder as well as D.A.V. Stow, as reviewers, for their very helpful comments that considerably improved the manuscript.

References

Anselmetti, F.S., Eberli, G.F., Ding, Z.-D., 2000. From the Great Bahama Bank into the Straits of Florida: a margin architecture controlled by sea-level fluctuations and ocean currents. Geol. Soc. Am. Bull. 112, 829–844.

Aubert, O., Droxler, A.W., 1992. General Cenozoic evolution of the Maldives carbonate system (equatorial Indian Ocean). In: Bulletin Centres Recherche Exploration Production Elf Aquitaine. vol. 16. pp. 113–136.

Aubert, O., Droxler, A.W., 1996. Seismic stratigraphy and depositional signatures of the Maldive Carbonate System (Indian Ocean). Mar. Pet. Geol. 13, 503–536.

Backman, J., Duncan, R.A., et al., 1988. Mascarene Plateau - sites 705–716. In: Proceedings of the Ocean Drilling Program, Initial Reports 115, College Station, TX.

Belopolsky, A., Droxler, A., 2003. Imaging Tertiary carbonate system - the Maldives, Indian Ocean: insights into carbonate sequence interpretation. Lead. Edge 22, 646–652.

Belopolsky, A.V., Droxler, A.W., 2004. Seismic expressions of prograding carbonate bank margins: middle Miocene, Maldives, Indian Ocean. In: Eberli, G.P., Masaferro, J.L., Sarg, J.F. (Eds.), Seismic Imaging of Carbonate Reservoirs and Systems, American Association Petroleum Geologists Memoir 81, Tulsa, pp. 267–290.

Betzler, C., Hübscher, C., Lindhorst, S., Reijmer, J.J.G., Römer, M., Droxler, A., Fürstenau, J., Lüdmann, T., 2009. Monsoon-induced partial carbonate platform drowning (Maldives, Indian Ocean). Geology 37, 867–870.

Betzler, C., Fürstenau, J., Lüdmann, T., Hübscher, C., Lindhorst, S., Paul, A., Reimer, J., Droxler, A.W., 2012. Sea-level and ocean-current control on carbonate platform growth, Maldives, Indian Ocean. Basin Res. 24, 1–15.

Betzler, C., Lüdmann, T., Hübscher, C., Fürstenau, J., 2013. Current and sea-level signals in periplatform ooze (Neogene, Maldives, Indian Ocean). Sediment. Geol. 290, 126–137.

Betzler, C., Lindhorst, S., Eberli, G.P., Lüdmann, T., Möbius, J., Ludwig, J., Schütter, I., Wunsch, M., Reijmer, J.J.G., Hübscher, C., 2014. Periplatform drift: the combined result of contour current and off-bank transport along carbonate platforms. Geology 42, 871–874.

Betzler, C., Lindhorst, S., Lüdmann, T., Weiss, B., Wunsch, M., Braga, J.C., 2015. The leaking bucket of a Maldives atoll: implications for the understanding of carbonate platform drowning. Mar. Geol. 366, 16–33.

Betzler, C., Eberli, G.P., Alvarez Zarikian, C.A., the Expedition 359 Scientists, 2016a. Expedition 359 Preliminary Report: Maldives Monsoon and Sea Level. International Ocean Discovery Program.http://dx.doi.org/10.14379/iodp.pr.359.2016.

Betzler, C., Eberli, G.P., Kroon, D., Wright, J.D., Swart, P.K., Nath, B.N., Alvvarez-Zarkikian, C.A., Alonso-Garcia, M., Bialik, O.M., Blatter, C.L., Guo, J.A., Haffen, S., Horozal, S., Inoue, M., Jovane, L., Lanci, L., Laya, J.C., Mee, A.L., Lüdmann, T., Nakakuni, M., Niino, K., Petruny, L.M., Pratiwi, S.D., Reijmer, J.J., Reolid, J., Slagle, A.L., Sloss, C.R., Su, X., Yao, Z., Young, J.R., 2016b. The abrupt onset of the modern South Asian Monsoon winds. Sci. Rep. 6, 29838.

Betzler, C., Hübscher, C., Lindhorst, S., Lüdmann, T., Reijmer, J.J.G., Braga, J.-C., 2016c. Lowstand wedges in carbonate platform slopes (Quaternary, Maldives, Indian Ocean). Depositional Rec. 2, 196–207.

Betzler, C., Eberli, G.P., Alvarez Zarikian, C.A., the Expedition 359 Scientists, 2017. Maldives monsoon and sea level. In: Proceedings of the International Ocean Discovery Program, 359: College Station, TX (International Ocean Discovery Program), http://dx.doi.org/10.14379/iodp.proc.359.2017.

Betzler, C., Eberli, G.P., Lüdmann, T., Reolid, J., Kroon, D., Reijmer, J.J.G., Swart, P.K., Wright, J., Young, J.R., Alvarez-Zarikian, C., Alonso-García, M., Bialik, O.M., Blättler, C.L., Guo, J.A., Haffen, S., Horozal, S., Inoue, M., Jovane, L., Lanci, L., Laya, J.C., Hui Mee, A.L., Nakakuni, M., Nath, B.N., Niino, K., Petruny, L.M., Pratiwi, S.D., Slagle, A.L., Sloss, C.R., Su, X., Yao, Z., 2018. Refinement of Miocene sea-level and monsoon events from the sedimentary record of the Maldives (Indian Ocean). Prog. Earth Planet. Sci. 5 (5). http://dx.doi.org/10.1186/s40645-018-0165-x.

Carter, L., McCave, I.N., 1994. Development of drift sediments approaching an active plate margin und the SW Pacific Deep Western Boundary Current. Paleoceanography 9 (6), 1061–1085.

Cartigny, M.J.B., Postma, G., van den Berg, J.H., Mastbergen, D.R., 2011. A comparative study of sediment waves and cyclic steps based on geometries, internal structures and numerical modeling. Mar. Geol. 280 (1–4), 40–56.

Cramer, B.S., Miller, K.G., Barrett, P.J., Wright, J.D., 2011. Late Cretaceous–Neogene trends in deep ocean temperature and continental ice volume: reconciling records of benthic foraminiferal geochemistry (δ^{18}O and Mg/Ca) with sea level history ocean overturning since the Late Cretaceous: inferences from a new benthic foraminiferal isotope compilation. J. Geophys. Res. 116. http://dx.doi.org/10.1029/2011JC007255.

Deptuck, M.E., Sylvester, Z., Pirmez, C., O'Byrne, C., 2007. Migration–aggradation history and 3-D seismic geomorphology of submarine channels in the Pleistocene Benin-major Canyon, western Niger Delta Slope. Mar. Pet. Geol. 24, 406–433.

Droxler, A.W., Schlager, W., 1985. Glacial versus interglacial sedimentation rates and turbidite frequency in the Bahamas. Geology 13, 799–802.

Eberli, G.P., Swart, P.K., Malone, M.J., et al., 1997. Proceedings ODP, Initial Reports 166, College Station, TX (Ocean Drilling Program).

Eberli, G.P., Anselmetti, F.S., Isern, A.R., Delius, H., 2010. Timing of changes in sea-level and currents along the Miocene platforms of the Marion Plateau, Australia. In: Morgan, W.A., George, A.D., Harris, P.M., Kupecz, J.A., Sarg, J.E. (Eds.), Cenozoic Carbonate Systems of Australasia by, Society for Sedimentary Geology Special Publication. vol. 95. pp. 219–242.

Faugères, J.-C., Stow, D.A.V., Imbert, P., Viana, A., 1999. Seismic features diagnostic of contourite drifts. Mar. Geol. 162, 1–38.

Faugères, J.-C., Zaragosi, S., Mézerais, M.L., Massé, L., 2002. The Vema contourite fan in the South Brasilian basin. In: Stow, D.A.V., Pudsey, C.J., Howe, J.A., Faugères, J.-C., Viana, A.R. (Eds.), Deep-water Contourite Systems: Modern Drifts and Ancient Series, Seismic and Sedimentary Characteristics, Geological Society London Memoir. vol. 22. pp. 209–238.

Gischler, E., Hudson, H.J., Pisera, A., 2008. Late Quaternary reef growth and sea level in the Maldives (Indian Ocean). Mar. Geol. 250, 104–113.

Hernández-Molina, F.J., Maldonado, A., Stow, D.A.V., 2008. Abyssal plain contourites. In: Rebesco, M., Camerlenghi, A. (Eds.), Contourites, Developments in Sedimentology. vol. 60. Elsevier, pp. 347–378.

Isern, A.R., Anselmetti, F.S., Blum, P., 2004. A neogene carbonate platform, slope, and shelf edifice shaped by sea-level and ocean currents, Marion Plateau (Northeast Australia). In: Eberli, G.P., Masferato, J.L., Sarg, J.F.R. (Eds.), Seismic Imaging of Carbonate Reservoirs and Systems, American Association Petroleum Geologists Memoir. vol. 81. pp. 291–307.

Janocko, M., Nemec, W., Henriksen, S., Warchol, M., 2013. The diversity of deep-water sinuous channel belts and slope valley-fill complexes. Mar. Pet. Geol. 41, 7–34.

Kench, P.S., Parnell, K.E., Brander, R.W., 2009. Monsoonally influenced circulation around coral reef islands and seasonal dynamics. Mar. Geol. 266, 91–108.

Knox, R.A., 1976. On a long series of measurements of Indian Ocean equatorial currents near Addu Atoll. Deep-Sea Res. 23, 211–221.

Kominz, M.A., Browning, J.V., Miller, K.G., Sugarman, P.J., Mizintseva, S., Scotese, C.R., 2008. Late Cretaceous to Miocene sea-level estimates from the New Jersey and Delaware coastal plain coreholes: an error analysis. Basin Res. 20, 211–226.

Locker, S.D., Laine, E.P., 1992. Paleogene-Neogene depositional history of the middle U.S. Atlantic continental rise: mixed turbidite and contourite depositional systems. Mar. Geol. 103, 137–164.

Lüdmann, T., Wiggershaus, S., Betzler, C., Hübscher, C., 2012. Southwest Mallorca Island: a cool-water carbonate margin dominated by drift deposition associated with giant mass wasting. Mar. Geol. 307-310, 73–87.

Lüdmann, T., Kalvelage, C., Betzler, C., Fürstenau, J., Hübscher, C., 2013. The Maldives, a giant isolated carbonate platform dominated by bottom currents. Mar. Pet. Geol. 43, 326–340.

McHargue, T., Pyrcz, M.J., Sullivan, M.D., Clark, J.D., Fildani, A., Romans, B.W., Covault, J.A., Levy, M., Posamentier, H.W., Drinkwater, N.J., 2011. Architecture of turbidite channel systems on the continental slope: patterns and predictions. Mar. Pet. Geol. 28, 728–743.

Mézerais, M.L., Faugères, J.-C., Figueiredo, A., Massé, L., 1993. Contour current accumulation off Vema Channel mouth, Southern Brazil basin. Sediment. Geol. 82 (1–4),

173–188.
Müller, D.R., Sdrolias, M., Gaina, C., Steinberger, B., Heine, C., 2008. Long-term sea-level fluctuations driven by ocean basin dynamics. Science 319, 1357–1362.
Phillips, E., 2006. Micromorphology of a debris flow deposit: evidence of basal shearing, hydro-fracturing, liquefaction and rotational deformation during emplacement. Quat. Sci. Rev. 25 (7–8), 720–738.
Purdy, E.G., Bertram, G.T., 1993. Carbonate concepts from the Maldives, Indian Ocean. In: American Association Petroleum Geologists Studies in Geology. vol. 34. pp. 56.
Rebesco, M., Camerlenghi, A., 2008. Contourites. Developments in Sedimentology. vol. 60. Elsevier, pp. 663.
Rebesco, M., Hernández-Molina, F.J., Van Rooij, D., Wåhlin, A., 2014. Contourites and associated sediments controlled by deep-water circulation processes: state-of-the-art and future considerations. Mar. Geol. 352, 111–154.
Schlager, W., 2005. Carbonate sedimentology and sequence stratigraphy. In: Concepts in Sedimentology and Paleontology. vol. 8. Society for Sedimentary Geology, pp. 200.
Schlager, W., Reijmer, J.J.G., Droxler, A., 1994. Highstand shedding of carbonate platforms. J. Sediment. Res. 64 (3), 270–281.
Storz, D., Gischler, E., 2011. Coral extension rates in the NW Indian Ocean I: reconstruction of 20th century SST variability and monsoon current strength. Geo-Mar. Lett. 31, 141–154.
Stow, D.A.V., Faugères, J.-C., 2008. Contourite facies and the facies model. In: Rebesco, M., Camerlenghi, A. (Eds.), Contourites, Developments in Sedimentology. vol. 60. Elsevier, pp. 223–256.
Stow, D.A.V., Faugères, J.-C., Howe, J.A., Pudsey, C.J., Viana, R., 2002a. Bottom currents, contourites and deep-sea sediment drifts: current state-of-the-art. In: Stow, D.A.V., Pudsey, C.J., Howe, J.A., Faugères, J.-C., Viana, A.R. (Eds.), Deep-water Contourite Systems: Modern Drifts and Ancient Series, Seismic and Sedimentary Characteristics. Geological Society London Memoir, vol. 22. pp. 7–20.
Stow, D.A.V., Pudsey, C.J., Howe, J.A., Faugères, J.-C., Viana, A.R., 2002b. Deep-water contourite systems: modern drifts and ancient series, seismic and sedimentary characteristics. In: Geological Society London Memoir. vol. 22. pp. 464.
Stow, D.A.V., Hunter, S., Wilkinson, D., Hernández-Molina, F.J., 2008. The nature of contourite deposition. In: Rebesco, M., Camerlenghi, A. (Eds.), Contourites, Developments in Sedimentology. vol. 60. Elsevier, pp. 143–155.
Viana, A.R., Rebesco, M., 2007. Economic and palaeoceanographic significance of contourite deposits. Geol. Soc. Lond., Spec. Publ. 276, 343.
Wetzel, A., Werner, F., Stow, D.A.V., 2008. Bioturbation and biogenic sedimentary structures in contourites. In: Rebesco, M., Camerlenghi, A. (Eds.), Contourites, Developments in Sedimentology. vol. 60. Elsevier, pp. 183–202.